# IMAGE RECONSTRUCTION IN COMPRESSED REMOTE SENSING WITH LOW-RANK AND $L_1$-NORM REGULARIZATION

*Jianwei Ma*

Institute of Applied Mathematics
Harbin Institute of Technology
Harbin 150001, China
jma@hit.edu.cn

*Yi Yang, Stanley Osher, Jerome Gilles*

Department of Mathematics
University of California, Los Angeles
CA 900095, USA
{yyang,sjo,jegilles}@math.ucla.edu

## ABSTRACT

In this paper, we proposed a new model with nuclear-norm and $L_1$-norm regularization for image reconstruction in aerospace remote sensing. The curvelet based $L_1$-norm regularization promotes sparse reconstruction, while the low-rank based nuclear-norm regularization leads to a principle component solution. Split Bregman method is used to solve this problem. Numerical experiments show the proposed model achieves better reconstruction results compared with the previous model with $L_1$-norm regularization.

***Index Terms***— Compressed remote sensing, low-rank, $L_1$-norm regularization, alternating direction method

## 1. INTRODUCTION

Remote sensing involves gathering data by the sensor, compressing, and transmitting the digital data back to a processing center. It has many important applications, e.g., imaging of the Earth's surface and ocean floors, assessment of crop conditions, deep-space exploration. Sensor systems, which may be airborne or satellite borne, are classified two categories. The first one is passive sensors, such as aerial photography, infrared imaging and passive microwave radiometers, that make use of natural radiation emitted or reflected by the object being observed. The second category is that of active sensors such as radars, altimeters and scatterometers. Based on the conventional imaging principle, millions of pixels captured by sensors have to be stored momentarily when we take pictures using a megapixel camera. How to increase storage and transmission efficiency without degrading picture quality is a challenging problem.

Recently, the idea of compressed sensing (CS) [1, 2] is applied in optical and radar remote sensing (renamed as compressed remote sensing (CRS) [14]). CS states that a compressible unknown signal can be recovered/reconstructed from incomplete sets of linear measurements by a specifically designed model. The CS imaging [3, 4, 5] can be implemented by single or multiple optical sensors, which not only saves the cost of additional sensors but also reduces the size and weight of onboard imaging instruments. CRS can save power consumption by avoiding the immediate compression step. The encoding captures the compressed form of a scene directly, which saves the computational cost of transmitting the data back to Earth from satellites within a limited bandwidth. Another potential advantage of CS imaging is that it can work much more easily in low light or outside the visible light spectrum due to the use of only one photon detector, hence it can be used for night vision and infrared imaging. It can lead to new instruments with simplified hardware, less storage space, less power consumption, and smaller size compared with the currently used charge-coupled device cameras. For imaging radars such as synthetic aperture radar (SAR) and inverse SAR (ISAR), CRS can again help to reduce data storage space as well as simplify the hardware (see e.g., [8, 9, 10, 11, 12]). CS can also lead to some specific applications such as moving target parameter estimation [13]. Most of CS applications in remote sensing can be divided into two categories [14]: 1) Parameter estimation and resolution improvement when the estimated parameter or the observed scene is sparse; 2) data compression or simpler hardware design.

Usually in CS model people use an $L_1$-norm term as regularizer. Nonconvex $L_p$-norm ($0 \leq p < 1$) has also been considered, which leads to sparser reconstruction results in most cases. In our previous RCS work [5, 6], we used $L_1$-norm of the curvelet coefficients of the objects as sparsity-promoting regularization.

Recently, low-rank promoting nuclear-norm regularization was successfully applied to matrix completion [17]. The regularization works very well when the object has a priori low rank. Thereafter, the low-rank idea has been applied in many fields such as video denoising [20], seismic data reconstruction [21], etc.

Combinations of the nuclear-norm and the $L_1$-norm terms

This work was partially supported by the Program for New Century Excellent Talents in University under Grant No. NCET-11-0804.

have been presented. In [18], the authors decomposed a given matrix into a low-rank component and a sparse component (named as robust principal component analysis: RPCA) by the so-called Principal Component Pursuit. The application of RPCA in the area of video surveillance has achieved promising results. Furthermore, the generalized rank, e.g., the matrix rank of tight frame transform of a multi-energy image, was considered for computed tomography (CT) [19]. It offers a way to characterize the multi-level and multi-filtered image coherence across the energy spectrum.

In this paper, we proposed a new decoding method for single-pixel CRS by combining the nuclear-norm and curvelet based $L_1$-norm regularization. The minimization of nuclear norm aims at reconstructing the low-rank principle components, and the minimization of $L_1$-norm promotes the reconstruction of sparse components. However, unlike RPCA which decomposes images into a low-rank part and a sparse part, our model applies the two regularization on the original image. Split Bregman algorithm is applied to solve the joint regularized minimization problem.

## 2. MATHEMATICAL MODEL

CS can be described mathematically as a fundamental problem of recovering a sparse signal $X$ of size $N \times 1$ from a small set of measurements $Y$. Let $A$ be a CS measurement matrix of size $K \times N$. Here, $K \ll N$, i.e., the rows of the measurement matrix are much fewer than the columns of the matrix. In practice, $A$ denotes a random binary masked lens in CRS. The encoding can be described as

$$Y = AX + \varepsilon, \tag{1}$$

where $\varepsilon$ denotes possible measurement errors or noise. Each element of $Y$ is a measurement acquired by a single sensor, i.e., the so-called single-pixel imaging [3]. The length of $Y$, $K$, means that the camera takes $K$-time measurements along the time sequence. Eq. (1) stands for the mathematical model of single-pixel multiple-time (SPMT) imaging. In this case, $A$ is a random binary matrix, which can be generated in practice by e.g., digital micro-mirror device (DMD) [3].

A popular model for $X$ recovery is the following:

$$\min_X \lambda|\varphi X|_1 + \frac{1}{2}||AX - Y||^2. \tag{2}$$

The first term in the above equation is a regularization term that represents a priori sparse information of the original scenes in certain space. The second term is a fidelity term that represents closeness of the solution to the observed scenes. $\varphi$ is a proper transform. $\lambda$ is a regularization parameter that can be tuned. In this paper, we use curvelet transform [15, 16] as $\varphi$. For images with line-like edges, its curvelet coefficients tend to be sparse. In this paper, we combine the low-rank regularization with our previous curvelet based $L_1$ regularization and propose the following joint model:

$$\min_X \lambda_1|\varphi X|_1 + \lambda_2||X||_* + \frac{1}{2}||AX - Y||^2. \tag{3}$$

Here $||X||_*$ denotes the nuclear norm of $X$, which is the $L_1$-norm of the singular values of $X$. It should be noted that the above model is a relaxation of the original sparse and low-rank regularized model

$$\min_X \lambda_1|\varphi X|_0 + \lambda_2 rank(X) + \frac{1}{2}||AX - Y||^2, \tag{4}$$

where the $rank(X)$ stands for $L_0$-norm of singular values of $X$. The (4) is an NP-hard problem that results from non-convexity and discontinuously of the objective function

## 3. MATHEMATICAL ALGORITHM

We apply split Bregman method, which is equivalent to ADMM (alternating direction method of multiplier), to solve the joint model (3). By introducing auxiliary splitting variables $D_1$ and $D_2$, (3) can be rewritten as

$$\begin{aligned} \min_X \lambda_1|D_1|_1 + \lambda_2||D_2||_* + \frac{1}{2}||AX - Y||^2, \\ s.t.\ \ D_1 = \varphi X,\ D_2 = X. \end{aligned} \tag{5}$$

By introducing Bregman iterative variables $B_1$ and $B_2$, we have the unconstrained minimization problem

$$\begin{aligned} &\min_X \lambda_1|D_1|_1 + \lambda_2||D_2||_* + \frac{1}{2}||AX - Y||^2 \\ &+\frac{\mu_1}{2}||D_1 - \varphi X - B_1||^2 + \frac{\mu_2}{2}||D_2 - X - B_2||^2. \end{aligned} \tag{6}$$

This problem can be solved by alternating direction method

$$\begin{aligned} D_1^{k+1} &= argmin_{d_1}\lambda_1|d_1|_1 \\ &\quad +\frac{\mu_1}{2}||d_1 - \varphi X^k - B_1^k||^2, && (7) \\ D_2^{k+1} &= argmin_{d_2}\lambda_2||d_2||_* \\ &\quad +\frac{\mu_2}{2}||d_2 - X^k - B_2^k||^2, && (8) \\ X^{k+1} &= argmin_X \frac{1}{2}||AX - Y||^2 \\ &\quad +\frac{\mu_1}{2}||D_1^{k+1} - \varphi X - B_1^k||^2 \\ &\quad +\frac{\mu_2}{2}||D_2^{k+1} - X - B_2^k||^2, && (9) \\ B_1^{k+1} &= B_1^k + \varphi X^{k+1} - D_1^{k+1}, && (10) \\ B_2^{k+1} &= B_2^k + X^{k+1} - D_2^{k+1}. && (11) \end{aligned}$$

The minimization problem in (7) can be solved by classical iterative thresholding, and the minimization in (8) can be solved by existing low-rank algorithms, e.g. iterative singular

value thresholding (SVT) [22], fixed point and Bregman iterations [23], nonlinear successive over-relaxation algorithm [24]. The minimization in (9) can be explicitly solved by

$$X = \beta^{-1}[A^T Y + \mu_1 \varphi^T (D_1^{k+1} - B_1^k) + \mu_2 (D_2^{k+1} - B_2^k)], \tag{12}$$

where

$$\beta = A^T A + (\mu_1 \varphi^T \varphi + \mu_2) I. \tag{13}$$

We have $\varphi^T \varphi = I$ for curvelet transform. If one takes orthogonal CS measurement matrix, i.e., $A^T A = I$, then $\beta = (1 + \mu_1 + \mu_2) I$.

## 4. NUMERICAL RESULTS

We apply 2D jittered sampling as the CS measurement matrix. Unlike the Gaussian random binary matrix, the jittered sampling controls that the maximal gap between ones should be smaller than a given value. In our test, we set $50\%$ elements as ones in the jittered binary matrix. We use parameters $\lambda_1 = 10$, $\lambda_2 = 20$, $\mu_1 = 0.02$, $\mu_2 = 0.02$, and 100 iterations. The SNR is computed by $10 \log_{10}(\|X\|_F^2 / \|X - X^*\|_F^2)$, where $X^*$ is the original scene and $X$ is the reconstructed one. Figure 1 shows a case of the single-pixel imaging of the Moon's surface. Figure 1 (a) is the original unknown scene. In this example, we consider white noise $\varepsilon = \rho M_Y R_N$ where the $\rho$ indicates the noise ratio, the $M_Y$ denotes the mean value of Y and $R_N$ denotes a $N \times 1$ vector of Gaussian random numbers. Figure 1 (b) shows a part of the CS matrix, where the white points denote ones. Figure 1 (c) and (d) are the reconstructed results by using curvelet $L_1$ regularized method [5] for different noise ratio $\rho = 0.001$ and $\rho = 0.002$, respectively. Figure 2 (e) and (f) show the reconstructed results by the proposed new method for the different noise ratio. Figure 2 (g) and (h) display the comparisons of their SNR (signal-to-noise ratio) as the number of iterations increases. With the help of the low-rank regularization, the proposed method obtains slightly better results than the previous $L_1$ method.

## 5. CONCLUSION

A joint low-rank and sparse promoting model is designed for signal reconstruction in the field of compressed remote sensing. Better reconstruction results can be obtained by the proposed model compared with previous curvelet based $L_1$ regularized model. This new model may be used for identification of moving targets when one reconstructs image sequence. Extension to radar imaging is our next work.

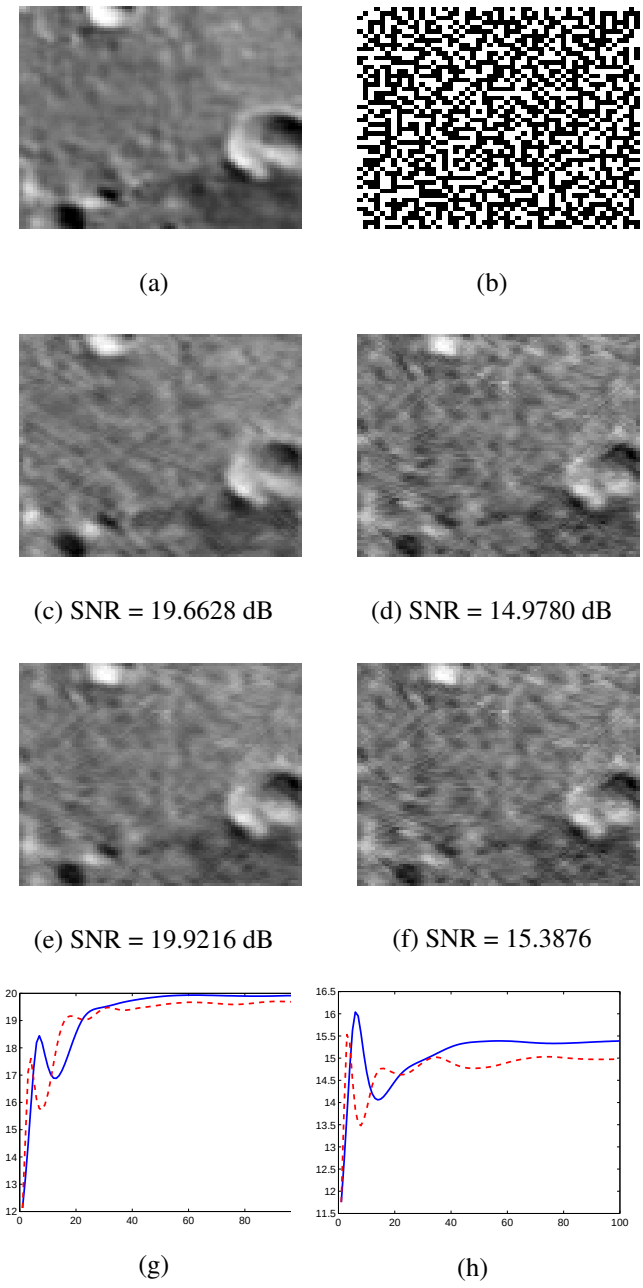


**Fig. 1**. (a) Original scene. (b) Part of jittered-sampling CS matrix. (c) and (d) Reconstruction by curvelet $L_1$ method for noise ratio $\rho = 0.001$ and $\rho = 0.002$, respectively. (e) and (f) Reconstruction by the proposed method for the different noise ratios. (g) (h) Comparisons of their SNR-vs-iteration curves. The solid lines denote the proposed method and dashed lines denote the curvelet $L_1$ method.

## 6. REFERENCES

[1] E. Candes, J. Romberg, and T. Tao, "Robust uncertainty principles: exact signal reconstruction from highly incomplete frequency information," IEEE Trans. Inform. Theory, vol. 52, no. 2, pp. 489-590, Feb. 2006.

[2] D. Donoho, "Compressed sensing," IEEE Trans. Inform. Theory, vol. 52, no. 4, pp. 1289-1306, April 2006.

[3] M. Duarte, M. Davenport, D. Takhar, J. Laska, T. Sun,

K. Kelly, and R. Baraniuk, "Single-pixel imaging via compressive sampling," IEEE Signal Process. Magazine, vol. 25, no. 2, pp. 83-91, March 2008.

[4] M. Neifeld and J. Ke, "Optical architectures for compressive imaging," Appl. Opt., vol. 46, no. 22, pp. 5293-5303, Aug. 2007.

[5] J. Ma, "Single-pixel remote sensing," IEEE Geosci. Remote Sens. Lett., vol. 6, no. 2, pp. 676-680, April 2009.

[6] J. Ma and F. Le Dimet, "Deblurring from highly incomplete measurements for remote sensing," IEEE Trans. Geosci. Remote Sensing, vol. 47, no. 3, pp. 792-802, March 2009.

[7] R. Marcia, R. Willett, and Z. Harmany, "Compressive optical imaging: architectures and algorithms," Optical and Digital Image Processing Fundamentals and Applications, edited by G. Cristobal, P. Schelkens and H. Thienpont, April 2010.

[8] M. Herman and T. Strohmer, "High-resolution radar via compressed sensing," IEEE Trans. Signal Process., vol. 57, no. 6, pp. 2275-2284, June 2009.

[9] J. Ender, "On compressive sensing applied to radar," Signal Process., vol. 90, no. 5, pp. 1402-1414, May 2010.

[10] V. Patel, G. Easley, D. Healy, and R. Chellappa, "Compressed synthetic aperture radar," IEEE J. Selected Topics in Signal Process., vol. 4, no. 2, pp. 244-254, April 2010.

[11] X. Zhu and R. Bamler, "Tomographic SAR inversion by l1-norm regularization: the compressive sensing approach," IEEE Trans. Geosci. Remote Sensing, vol. 48, no. 10, pp. 3839-3846, Oct. 2010.

[12] L. Potter, E. Ertin, J. Parker, and M. Cetin, "Sparsity and compressed sensing in radar imaging," Proceedings of the IEEE, vol. 98, no. 6, pp. 1006-1020, June 2010.

[13] A. Khwaja and J. Ma, "Applications of compressed sensing for SAR moving target velocity estimation and image compression," IEEE Trans. Instrumentation and Measurement, vol. 60, no. 8, pp. 2828-2860, Aug. 2011.

[14] J. Ma, A. Khwaja, and M. Hussaini, "Compressed remote sensing, in Signal and Image Processing for Remote Sensing," edited by Chi H. Chen, the second version, pp. 73-90, Feb. 2012.

[15] E. Candes, L. Demanet, D. Donoho, and L. Ying, "Fast discrete curvelet transforms," Multiscale Model. Simul., vol. 5, no. 3, pp. 861-899, Sep. 2006.

[16] J. Ma and G. Plonka, "The curvelet transform," IEEE Signal Process. Magazine, vol. 27, no. 2, pp. 118-133, March 2010.

[17] E. Candes and B. Recht, "Exact matrix completion via convex optimization," Found. of Comput. Math., vol. 9, no. 6, pp. 717-772, April 2009.

[18] E. Candes, X. Li, Y. Ma, and J. Wright, "Robust Principal Component Analysis?," Journal of the ACM, vol. 58, no. 3, pp. 1-37, Dec. 2011.

[19] H. Gao, H. Yu, S. Osher, and G. Wang, "Multi-energy CT based on a prior rank, intensity and sparsity model (PRISM)", Inverse Problems, vol. 27, no. 11, pp. 115012-115033, Nov. 2011.

[20] H. Ji, C. Liu, Z. Shen, and Y. Xu, "Robust video denoising using low rank matrix completion," In Computer Vision and Pattern Recognition (CVPR), 2010 IEEE Conference, June 2010.

[21] Y. Yang, J. Ma, and S. Osher, "Seismic data reconstruction via matrix completion," UCLA CAM Report 12-14, Feb. 2012.

[22] J. Cai, E. Candes, and Z. Shen, "A singular value thresholding algorithm for matrix completion," SIAM J. Optimization, vol. 20, pp. 1956-1982, Oct. 2010.

[23] S. Ma, D. Goldfarb, and L. Chen, "Fixed point and Bregman iterative methods for matrix rank minimization," Mathematical Programming, vol. 128, pp. 312-353, Sep. 2011.

[24] Z. Wen, W. Yin, and Y. Zhang, "Solving a low-rank factorization model for matrix completion by a nonlinear successive over-relaxation algorithm," Rice CAAM Report TR10-07, 2010.